NASA Technical Memorandum 102310
AIAA-89-2840

Investigation of a Liquid-Fed Water Resistojet Plume

D.H. Manzella
Sverdrup Technology, Inc.
NASA Lewis Research Center Group
Cleveland, Ohio

and

L.M. Carney
National Aeronautics and Space Administration
Lewis Research Center
Cleveland, Ohio

Prepared for the
25th Joint Propulsion Conference
cosponsored by the AIAA, ASME, SAE, and ASEE
Monterey, California, July 10-12, 1989

NASA

INVESTIGATION OF A LIQUID-FED WATER RESISTOJET PLUME

D.H. Manzella
Sverdrup Technology, Inc.
NASA Lewis Research Center Group
Cleveland, Ohio 44135

and

L.M. Carney
National Aeronautics and Space Administration
Lewis Research Center
Cleveland, Ohio 44135

ABSTRACT

Measurements of mass flux and flow angle were taken throughout the forward flow region of the exhaust of a liquid-fed water resistojet using a quartz crystal microbalance (QCM). The resistojet operated at a mass flow rate of 0.1 g/s with a power input of 330 Watts. Measured values were compared to theoretical predictions obtained by employing a source flow approximation. Excellent agreement between predicted and measured mass flux values was attained; however, this agreement was highly dependent on knowledge of nozzle flow conditions. Measurements of the temperature at which the exhaust condensed on the QCM were obtained as a function of incident mass flux.

INTRODUCTION

Recently, there has been renewed interest in resistojets capable of utilizing water as a propellant. The multipropellant resistojet baselined for Space Station Freedom will potentially use water as a propellant.[1] Also, the commercially-sponsored, man-tended space platform recently considered for development baselined water resistojets as the primary on-orbit propulsion.[2] Resistojet thrusters have been successfully integrated into spacecraft dating back to 1965,[3] and although water was a candidate propellant for the biowaste resistojets of the Manned Orbital Research Laboratory (MORL) proposed in the early 1970's,[4] a liquid-fed water resistojet has not been flight tested.

Successful integration of the water resistojet requires an accurate assessment of the potential impact that the water vapor plume may have on the spacecraft operation and missions. Since water vapor is readily condensible, one impact of primary concern is the possible contamination of spacecraft surfaces due to mass deposition. Sensitive optical surfaces, solar arrays, and thermal control surfaces can be adversely affected by the deposition of even a few angstroms of water. Field of view interferences caused by environmental contamination are also a concern for spacecraft users. Other potential impacts which must be addressed include thrust losses, disturbance torques, or thermal loading due to plume impingement. The magnitude of these impacts are highly dependent on the spacecraft architecture.

To predict the potential contamination effects of a water resistojet propulsion system, the plume must be modeled analytically, and, where possible, verified experimentally. A complete analysis of the exhaust flow field requires a solution to the Boltzmann equation. With the advent of supercomputers, great progress has been made in obtaining approximate numerical solutions of exhaust plumes using methods such as the Method of Characteristics (MOC),[5,6] Direct Simulation Monte Carlo (DSMC)[7,8] and kinetic theory models.[9,10] G.A. Simons presented a widely used source flow method for the prediction of rocket exhausts.[11] This method accounts for the expansion of the supersonic portion of the boundary layer of the nozzle, along with the inviscid core. Plume properties are expressed in terms of conditions at the nozzle exit and in terms of the boundary layer thickness. As this method was primarily devoted to the prediction of high thrust rocket nozzles with very thin boundary layers, there was no provision for subsonic boundary layer expansion. This method has been successfully utilized in the past by Genovese[12] to predict spacecraft/plume interactions. Agreement between values calculated for a hydrazine monopropellant thruster plume interacting with a solar array and actual flight data was good. Calia and Brook[13] also found good agreement with mass flux measurements made at large angles from the plume centerline of a small-scale reaction control engine.

Experimental verification of any of the above-mentioned techniques in a ground-based facility is a difficult task as it is not possible to accurately simulate the space environment while the thruster is operational. However, meaningful plume data can be obtained in the forward region of the plume (downstream of the nozzle exit plane) at facility pressures less than 10^{-4} Torr for condensable propellants with the use of cryogens such as gaseous Helium at 16 K (GHe) or liquid Nitrogen at 77 K (LN_2). A number of diagnostic techniques for the measurement of plume properties are well established. Experimental studies[14,15] of pure gas, conical nozzle expansions into hard vacuum have been made to investigate the effects of nozzle area ratio and lip geometry, facility pressure, propellant condensation, and inadequate cryopumping in the back flux region.

Preliminary investigations of the resistojet thruster plume have been reported by Zana, et al.[16] They made a comparison between mass flux measurements taken with a QCM and predicted values using a modified version of Simons' method. Because the resistojet thruster is characterized by highly viscous flow in very small nozzle geometries, the method of Simons' was modified by Hoffman[17] to account for the thick boundary layers present in the nozzle. The mass flux data were obtained in the exhaust of a laboratory model resistojet operating on unheated CO_2 using a cryogenically-cooled quartz crystal microbalance (QCM). In order to avoid limitations in the dynamic range of the QCM, a small amount of H_20 in the CO_2 was used as a tracer of the actual flow field. Qualitative agreement between theoretical predictions and experiment was found in the forward flux region. Breyley, et al.[18] conducted a similar investigation addressing the effect of nozzle geometry on the exhaust plume. Again, agreement between the modified Simons' method and experiment proved to be qualitative. Both studies indicated that the suitability of the modified Simons' technique for predicting the exhaust flow field of viscous, low-thrust nozzles was promising but further experimental data were needed.

The objective of this work was to experimentally map the exhaust flow field of a liquid-fed, water resistojet and identify potential plume effects on a spacecraft with the primary focus on contamination. A cryogenically-cooled quartz crystal microbalance was used to obtain a mapping of mass flux in the forward flux region of the plume. Also, local deposition rates as a function of surface temperature were obtained at various locations in the plume. In addition, an analytical study using the modified Simons' method for predicting the forward flow plume was conducted and compared to experimental measurements.

This paper briefly describes the modified Simons' method and provides details of the measurement technique and experimental hardware. The QCM response during data collection as a function of time and crystal temperature is described. Profiles of measured mass flux as a function of QCM angular orientation with the flow streamlines are presented. The measured mass flux data are then compared with the plume density calculations based on the modified Simons' method. The sensitivity of the analysis to the selection of major plume parameters used in the calculations is also discussed.

SYMBOLS

A	plume normalization constant
$f(\theta)$	angular density variation
k	QCM constant, g·Hz
m	mass, g
R^*	nozzle throat radius, cm
r	spherical radius, cm
r_e	nozzle exit radius, cm
U_e	nozzle exit plane velocity, m/s
U_{lim}	limiting velocity, m/s
$\bar{U}_{lim}$	limiting velocity in the boundary layer, m/s
x_e	distance along nozzle wall to exit, cm
α	ratio between U_{lim} and $\bar{U}_{lim}$
β	plume parameter
γ	specific heat ratio
δ_e	boundary layer thickness, cm
θ	angle from plume centerline, degrees
θ_{noz}	nozzle half angle, degrees
θ_o	angle to edge of boundary layer, degrees
θ_∞	limiting turning angle, degrees
κ	simpification for β determination, Eq.*(8)*
μ	viscosity, N·s/m^2
ν	Prandtl-Meyer limiting angle, degrees
ν_{max}	maximum Prandtl-Meyer limiting angle, degrees
ρ	density, g/cm^3
ρ^*	nozzle throat density, g/cm^3
ω	natural resonant frequency of sensor crystal, Hz

ANALYSES

The modified Simons' method was chosen as the method of analysis because of its simplicity and ease of implementation. It is a semi-empirical, far-field approximation based on the more rigorous numerical solutions. This section summarizes the equations used to describe the plume flow field. Detailed discussions of the rationale and methodology of Simons' method and later modifications of Hoffman may be found in Refs. 11 and 17, respectively.

In the far field, rocket nozzle flow may be treated as though it originates from a point source. The plume structure, however, may be divided into two distinct regions: the region which originates in the inviscid core of the nozzle, and the region which originates in the supersonic boundary layer. Using continuity, the density at any point in the plume can be calculated in closed form based on conditions in the nozzle according to the following equation:

$$\rho/\rho^* = A(R^*/r)^2 f(\theta) \qquad (1)$$

The density varies inversely as the square of the distance from the thruster,and is related to the centerline value by a function $f(\theta)$. This angular variation is described by two different expressions. The first expression is applicable for angles less than θ_o, the limiting turning angle for the plume's inviscid core. In this part of the plume the density is modeled by a cosine power function:

$$f(\theta) = \left[\cos\left(\frac{\pi\theta}{2\theta_\infty}\right)\right]^{\frac{2}{\gamma-1}} \qquad 0 \le \theta \le \theta_o \qquad (2)$$

The second expression for the angular density variation is applicable in the outer region of the plume resulting from the expansion of the supersonic portion of the boundary layer; the subsonic portion of the boundary layer is neglected in this analysis. This corresponds to angles between θ_o and θ_∞. In this region the model predicts that the density drops off exponentially:

$$f(\theta) = f(\theta_o)\, exp\left[-\beta(\theta - \theta_o)\right] \qquad \theta_o < \theta \le \theta_\infty \qquad (3)$$

There is no provision for flow beyond the calculated limiting turning angle, θ_∞. The plume normalization constant in equation *(1)* is calculated using the following expression which is a simplification based on inviscid theory:

$$A = \frac{1}{8}\left[\frac{\gamma+1}{\gamma-1}\right]^{1/2}\left[\frac{\pi}{\theta_\infty}\right]^2 \qquad (4)$$

The limiting turning angle, θ_∞, may be calculated with the following expression:

$$\theta_\infty = \nu_{max} - \nu + \theta_{noz} \qquad (5)$$

where ν_{max} is the limiting expansion angle for a flow with an infinite Mach number, ν is the limiting expansion angle for a flow with the nozzle exit plane Mach number, and θ_{noz} is the geometric nozzle half angle. The remaining parameters θ_o and β are functions of the nozzle exit conditions and the boundary layer thickness:

$$\theta_o = \theta_\infty \frac{2}{\pi}\cos^{-1}\left[\frac{\delta_e}{r_e}\left(2 - \frac{\delta_e}{r_e}\right)^{\frac{\gamma+1}{\gamma-1}}\right] \qquad (6)$$

$$\beta = \frac{\kappa}{2}\sin\theta_o + \sqrt{\frac{\kappa^2}{4}\sin^2\theta_o + \kappa\cos\theta_o - 1} \qquad (7)$$

where κ is:

$$\kappa = A\left(\frac{\gamma+1}{\gamma-1}\right)^{1/2}\frac{2\bar{U}_{lim}}{U_{lim}}\left[\frac{\delta_e}{r_e}\left(2 - \frac{\delta_e}{r_e}\right)\right]^{\frac{1-\gamma}{1+\gamma}} \qquad (8)$$

and $\bar{U}_{lim} = \alpha U_{lim}$ and $0.5 \le \alpha \le 1.0$. The boundary layer thickness, δ_e, is calculated using a classical flat plate analysis for laminar flow from Schlichting.[19]

$$\delta_e \approx \sqrt{\frac{\mu x_e}{\bar{U}_e}} \qquad (9)$$

APPARATUS

Test Facility

The experimental investigation was conducted in Tank 5 of the Electric Power Laboratory at the NASA Lewis Research Center. The cylindrical vacuum chamber is 18 m long and 5 m in diameter. The pumping system consists of twenty, 0.8 m diameter oil diffusion pumps with four rotary lobe-type blowers and four rotating piston roughing pumps installed in parallel. The facility is also cryogenically pumped with two large cryopanels installed at one end of the chamber (Fig. 1). The panels were LN_2-cooled to temperatures less than 90 K prior to testing. This portion of the tank was separated from the remainder of the tank by an auxiliary baffle and movable louvers. These louvers were in the open position during operation.

The thruster was located 0.2 m from the tank wall and was oriented such that it exhausted along an axis perpendicular to the tank's major axis. Tank pressures were monitored at three different locations during operation using hot-cathode ionization gauges. During thruster operation the tank pressure ranged from $1x10^{-5}$ Torr near the cryopanels to $7x10^{-5}$ Torr directly across from the resistojet.

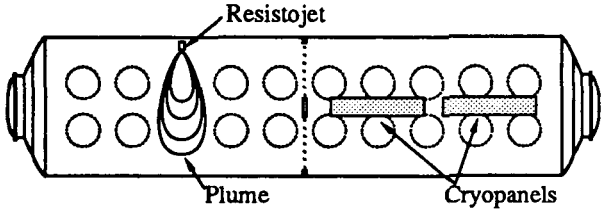

Figure 1. - Tank 5 including resistojet and cryopanels

Thruster

The water resistojet employed for this study was a first generation thruster developed during an on-going research program at the NASA Lewis Research Center. A complete performance characterization of this device was conducted by Morren and Stone.[20] Fig. 2 displays a cross sectional schematic of the resistojet. The major components of this thruster were fabricated from stainless steel, while the helical heating coil was constructed from an insulated nichrome wire. The converging-diverging nozzle had a twenty degree half angle, a throat diameter of 0.012 cm, and an expansion ratio of 100:1.

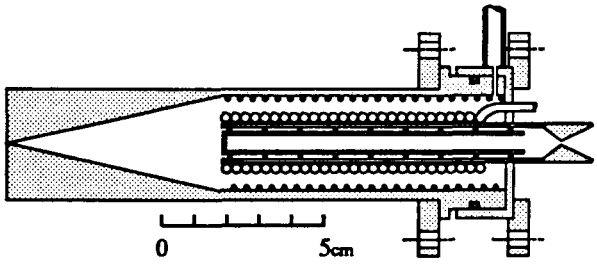

Figure 2. - First Generation Liquid-Fed Water Resistojet

Quartz Crystal Microbalance

Mass flux measurements were taken in various parts of the plume using a cryogenically-cooled quartz crystal microbalance (QCM). QCMs have been used in similar investigations of exhaust flow fields.[14-16,18,21] The QCM is a simple intrusive diagnostic tool consisting of a matched pair of precision crystals which oscillate at 10 MHz. The two crystals are LN_2-cooled to temperatures sufficient to condense mass on one of the crystals (sensor crystal). The other crystal serves as a reference and is not exposed to the incident mass flux. As mass condenses on the exposed surface of a sensor crystal the frequency of the oscillation changes according to the following relationship:

$$\Delta\omega = \Delta m\,(\omega^2/k) \qquad (10)$$

where ω is the natural resonant frequency of the crystal, k is a constant dependent on the crystal cut, and Δm is the change in mass. The difference between the two frequencies, the beat frequency, which is directly proportional to the incident mass flux, was monitored using a digital meter. Pertinent operating characteristics and dimensions of the QCM may be found in Table I.

Table I - Characteristics of QCM

Crystal Frequency, MHz	10
Mass Sensitivity, $g/cm^2 \cdot s$	$4.5x10^{-9}$
Operating Temperature, K	10 - 360
Beat Frequency Output, kHz	0 - 100
Crystal Collection Area, cm^2	0.3167
Outer Dimensions, cm	0.318 dia x 3.18

The QCM was mounted on an actuator system capable of being translated linearly in directions both parallel and perpendicular to the thrust axis as shown in Fig. 3. The QCM could also be rotated about its centerline with a rotary actuator. Axially, the QCM could be positioned between 20 and 120 cm from the thruster exit plane. Radially, the QCM could be positioned ±42 cm relative to the thrust axis. The QCM could also be rotated±90 degrees with respect to the thrust axis. A rotary angle of zero degrees corresponds to a parallel alignment of the normal to the QCM crystal surface with the thrust axis. The linear positional accuracy was estimated to be within ±0.2 cm and the rotational accuracy was estimated to be within ±0.2 degrees.

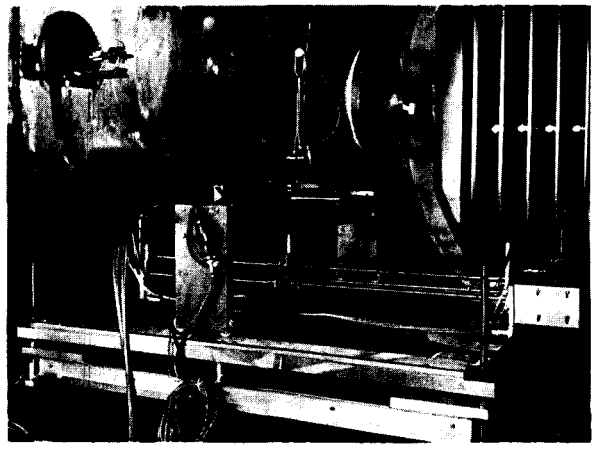

Figure 3. - Probe Actuator System

PROCEDURE

The experiment was designed to map the plume produced by a liquid-fed water resistojet. The thruster was operated at a nominal mass flow rate of 0.10 g/s and a power input of 330 Watts. Additional performance data are given in Table II. The reported value of thrust is from measurements taken by Morren and Stone.[18] Performance of this thruster was found to be stable and repeatable. In the current investigation, the mass flow rate, heater voltage, heater current and five internal temperatures were monitored routinely during operation.

Table II - Water Resistojet Performance Data

Feed Pressure, KPa	667
Voltage, volts	43.9
Current, amps	7.5
Power, Watts	330
Mass Flow Rate, mg/s	102
Thrust, mN	170
Specific Impulse, s	170
Heater Temperature, K	
inlet	1020
middle	1005
exit	1018

In all tests the resistojet was run until stable operation was achieved. At this point, the QCM was positioned at the location of interest and LN_2 flow through the cooling lines was initiated. At a particular temperature mass began to collect on the sensor crystal. This initial condensation temperature was recorded. The amount of mass collected, the mass rate of change and the QCM temperature were recorded digitally using a computer once every second. Once the rate of mass collection stabilized the QCM was rotated. The rate of mass collection was monitored until constant and the QCM was again rotated. This procedure was repeated until the sensor crystal was saturated. It was assumed that once mass started condensing on the crystal at a constant rate, there was no further temperature dependance. The QCM response at six different angular positions and the QCM temperature are plotted as a function of time in Fig. 4. Each cluster of data points was taken at a different angular orientation. After saturating the sensor crystal, the LN_2 flow to the cooling line was discontinued, the surface of the crystal was heated until clean, and the entire procedure was repeated. The reproducibility of the measured mass rate of change at a point was within ±5 percent.

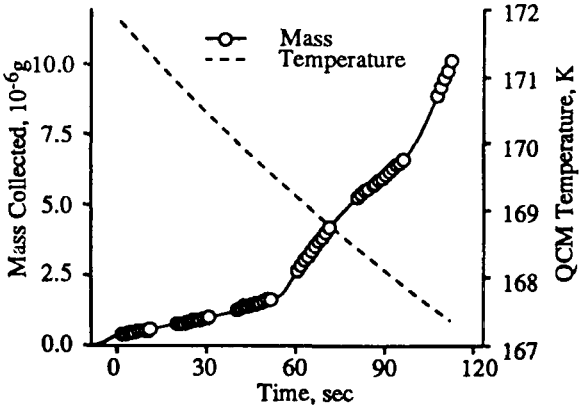

Figure 4. - QCM Response

To determine the mass flux at any location in the plume from the measured mass collection rate a capture coefficient must be considered. The capture coefficient is defined as the fraction of impinging molecules which adhere to the surface of the crystal. For this investigation a capture coefficient of 1.0 (independent of the rate of incidence on the surface) was assumed for simplicity. Values as low as 0.92 have been observed for H_2O condensing on a 77 K surface.[22] Mass flux values were determined at approximately sixty locations in the resistojet flow field. Rotary variation in mass flux as a function of the QCM angular orientation was determined at forty of these locations.

In addition to rotary surveys, measurements were taken with the QCM at a fixed angular orientation. These measurements were taken along three radial lines originating from the center of the nozzle exit plane at angles of 0, 10, and 20 degrees from centerline. The QCM was moved to a position along one of the lines and oriented at an angle of 70 degrees with respect to the line (see Fig. 5). When the QCM was in position, LN_2 flow was initiated and the sensor cooled. When the rate of collection stabilized, the mass flux was recorded. If the sensor crystal was not saturated after obtaining a stable mass flux reading the QCM was moved to a new position along the radial line (still oriented at a 70 degree angle with respect to the line) and additional mass flux measurements were taken. If the crystal was saturated, the heating/cooling cycle had to be repeated.

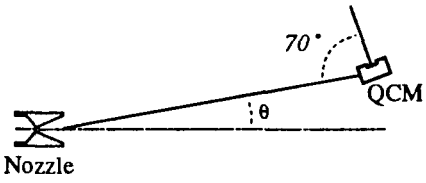

Figure 5. - QCM Orientation for Fixed Angle Measurements

The mass flux measured by a rotary QCM has been found to exhibit a cosine variation about the streamline.[12,13] By utilizing this relationship and only measuring a small component of the total mass flux, the limit in the dynamic range of the QCM could be avoided. Mass flux measurements taken at a known angle with respect to a particular streamline could be corrected to give the mass flux that would have been measured along the streamline at that location in the plume. Using this procedure, measurements were obtained as close as 35 cm on centerline from the thruster. The existence of this cosine variation centered about the direction of the radial lines was subsequently verified at a minimum of one position along each of the three lines by conducting a complete rotary survey. The uncertainty in any of the mass flux measurements was estimated to be within ± 30 percent primarily due to the temperature dependence of the capture coefficient.

RESULTS AND DISCUSSION

The QCM was used to experimentally map the plume produced by a liquid-fed water resistojet. The data were compared to theoretical predictions obtained using the modified Simons' method, and the sensitivity of the modified Simons' source flow approximation to selection of two critical plume parameters was considered.

QCM Measurements

As expected, the condensation temperatures were found to depend on the magnitude of the incident mass flux. Fig. 6 is a plot of condensation temperature versus the steady state mass flux measured at many different QCM positions and orientations. The variation is uniform and the results were repeatable. This result indicates that the amount of condensation of water vapor from a resistojet on sensitive spacecraft surfaces can be successfully addressed experimentally. By placing a QCM at the location of interest relative to the resistojet, surface temperatures below which condensation would occur can be determined.

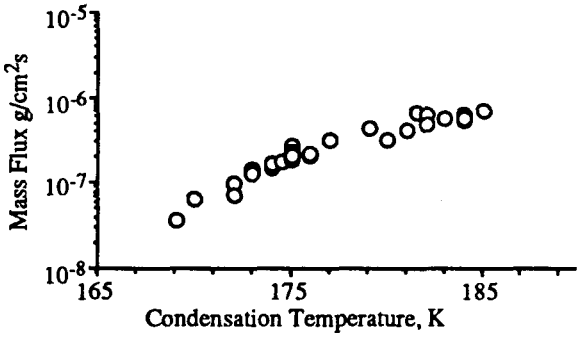

Figure 6. - Mass flux vs. Condensation Temperature

As previously stated, mass flux measurements were taken as a function of QCM angle at over forty different locations. These rotary surveys demonstrated a cosine variation centered on the streamline. A typical profile is shown in Fig. 7(a) where an angle of zero degrees denotes parallel alignment of the QCM surface normal with the thrust axis. The existence of this cosine distribution is easily understood by considering the geometry of the fluid-QCM interaction. At any particular orientation, the mass condensing on the sensor crystal was due to both the directed molecules of the exhaust and randomly directed molecules resulting from collisions. When the surface of the sensor crystal is aligned perpendicular to the flow streamline the maximum number of directed molecules impinges on the surface. As the orientation of the QCM changes, the molecules moving in the direction of the streamline have a smaller projected area of the sensor crystal to condense on since the projected area varies with the cosine of the angle. The mass flux resulting from the randomly directed molecules was sufficiently low in comparison to the mass flux resulting from the exhaust throughout the forward flow region of the plume. For the measured profile in Fig. 7(a) the measured local flow angle occurred at -40 degrees with respect to the thrust axis.

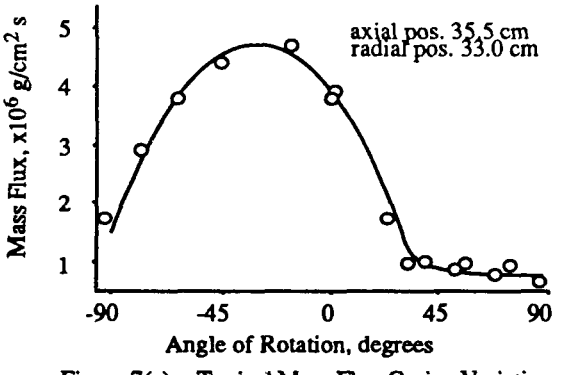

Figure 7(a). - Typical Mass Flux Cosine Variation

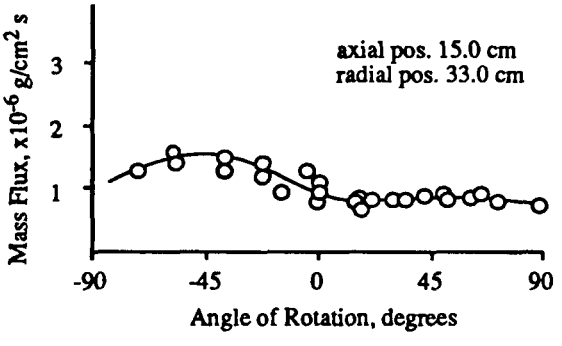

Figure 7(b). - Mass Flux Variation Near Background Values

The variation in mass flux with angle is shown in Fig. 7(b) for a location in which the magnitude of the mass flux resulting from the directed molecules of the plume was approaching background values. The interaction between the directed molecules of the plume and the randomly directed molecules that have undergone collisions resulted in a cosine variation that approached the uncertainty of the measurements. The characteristic cosine variation was still evident, but the maximum measured mass flux was only 40 percent higher than the mass flux values measured perpendicular to the measured streamline of -45 degrees.

From the rotary surveys, the local streamlines were determined at each location by curve-fitting a cosine to the measured mass flux values as shown in Fig 7. The relative magnitude of the on-streamline mass flux and the direction of the streamline are plotted in Fig. 8. The magnitude of the mass flux and the flow angle on both sides of the thrust centerline were approximately equal indicating that the plume was symmetric. However, there was a variation in the background mass flux measured at 90 degrees to the streamlines on either side of the thrust axis. Measurements taken on the side of the plume nearest the LN_2 cooled cryopanels consistently resulted in a lower measured background mass flux. The difference in the measured background mass flux as a function of location in the tank was indicative of facility interaction. During prolonged runs it became evident that a significant portion of the total amount of water exhausted into the vacuum chamber had been collected on the LN_2 cooled cryopanels. Therefore, the difference in measured background mass fluxes reflected the existence of a density gradient along the length of the tank caused by an asymmetry in the pumping system with respect to the resistojet exhaust. Three ionization gauges placed at different locations within the vacuum chamber also verified the existence of a density gradient. The ionization gauge closest to the cryopanels consistently indicated a lower tank pressure ($1x10^{-5}$ Torr) while the resistojet was operating.

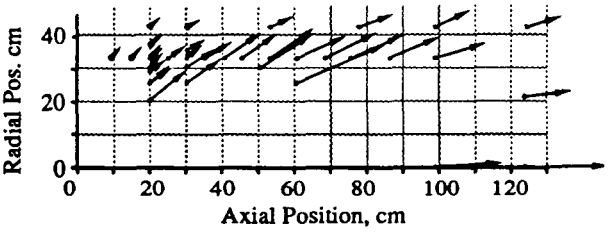

Figure 8. - Mass Flux Vectors from Rotary Surveys

The magnitude of the mass flux vectors determined from the rotary surveys reached a low of $1.3x10^{-6}$ g/cm²s at a location 10 cm downstream of the nozzle exit and 33 cm off the centerline. The maximum mass flux measured at angles greater than 45 degrees from the thrust axis was $2.7x10^{-6}$ g/cm²s. A background mass flux of $4.6x10^{-6}$ g/cm²s was calculated based on the assumption of randomly directed ambient temperature molecules at a pressure of $7x10^{-5}$ Torr. This pressure was measured with an ionization gauge on the tank wall directly opposite the resistojet. The differences between the calculated background mass flux and the measured mass fluxes also indicated that a significant density gradient existed in the vacuum chamber.

A consideration of these facility effects has been included because measurements of plume properties taken in vacuum facilities are strongly dependent on the ability of a facility to accurately simulate a space environment. It was

recognized that meaningful measurements could not be obtained in all regions of the plume in the facility used for these tests. Those measurements taken in lower density regions of the plume have a higher degree of uncertainty than those taken in higher density regions; however, no measurements were taken where facility effects were thought to predominate over the expansion process. Consequently, no data were obtained at high angles from the centerline (near 90 degrees).

No rotary surveys were taken near the plume centerline because the water molecules from the exhaust condensed on the sensing crystal at such a rapid rate that the dynamic range of the device was quickly exceeded. In many cases the condensed layer of water molecules was so thick it prevented the crystal from oscillating at all. As previously mentioned, to avoid these limitations, the cosine relationship with rotary angle was employed. The QCM was oriented at a particular angle to a radial line and the measured value was corrected assuming the radial line was a streamline. The radial lines were experimentally verified to be streamlines by taking rotary surveys at a minimum of one point along each line. The resulting measured streamline angles determined along radial lines 0, 10, and 20 degrees relative to the thrust axis are included in Fig. 8.

Fixed angle mass flux measurements were taken along the plume centerline. The QCM was oriented at an angle of 70 degrees to the plume centerline. The centerline mass flux was then calculated assuming a cosine distribution centered at zero degrees. These values are presented in Fig. 9. A $1/r^2$ relation was fit to the experimental data. The small scatter in the data relative to the $1/r^2$ curve demonstrates the reliability of the QCM measurements.

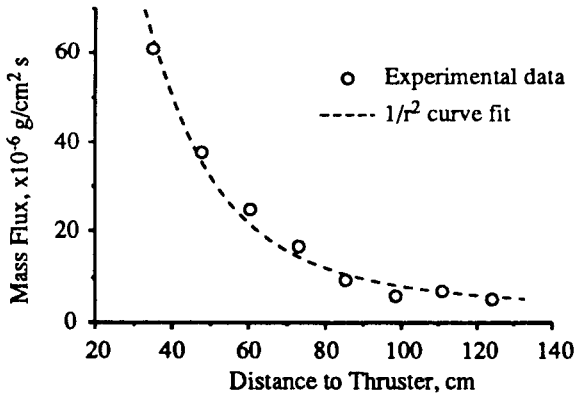

Figure 9. - Centerline Mass Flux

Parametric Analyses

The modified version of Simons' method was used to obtain the number density distribution in the resistojet plume. As discussed previously, the density distribution in the plume is functionally dependent on several critical parameters which require a knowledge of conditions at the nozzle throat and exit plane. An accurate value of the normalizing throat density is required for an absolute magnitude of number density in the plume. For this analysis, the throat density was based on a one-dimensional, isentropic analysis of the nozzle using the measured thrust and stagnation pressure to calculate a stagnation temperature at the throat. A throat density was then calculated from ideal gas dynamic relations. To account for real gas effects such as viscous dissipation in the nozzle, a 92 percent nozzle efficiency was assumed and the ideal throat density was increased by 8 percent for the analysis.

Fig. 10 displays the parametric sensitivity of the modified Simons' method to θ_∞, δ_e and α for a given set of conditions. The thruster nozzle exit plane is located at the origin. In the figures, the plotted contour represents a number density of 10^{12} molecules/cm^3. Marked differences in the calculated number density were observed for varied parameters holding all else constant. For example, the selection of the limiting turning angle is calculated from a knowledge of specific heat ratio and the Mach number at the exit plane (Eq. *(5)*). For the resistojet operating on H_2O with a γ of 1.33, an exit plane Mach number of 6.1 was calculated from isentropic flow relations. This gives a calculated limiting turning angle of 74 degrees. However, previous experimental data indicates that the flow extends beyond the calculated limiting turning angle.[16] . This is characteristic of low Reynolds Number nozzle flows which have large boundary layers. Again, this analysis neglected the expansion of the subsonic portion of boundary layer. Fig. 10(a) presents number density contours for limiting angles of 74°, 105°, and 135°.

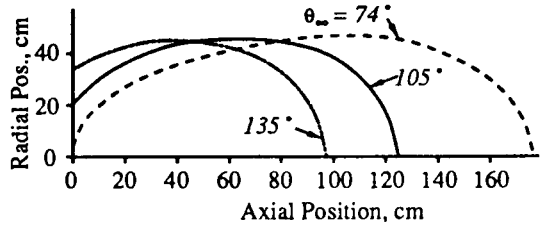

Figure 10(a). - Variation in 1.0×10^{12} mol/cm^3 number density contour with the limiting turning angle, θ_∞

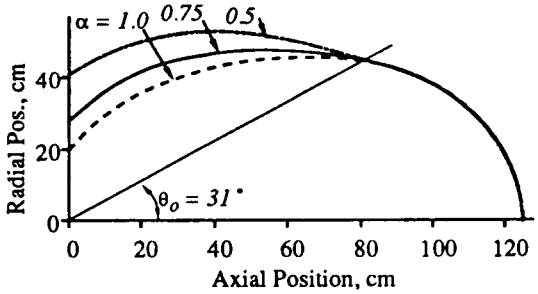

Figure 10(b). - Variation in 1.0×10^{12} mol/cm^3 number density contour with the plume parameter, α

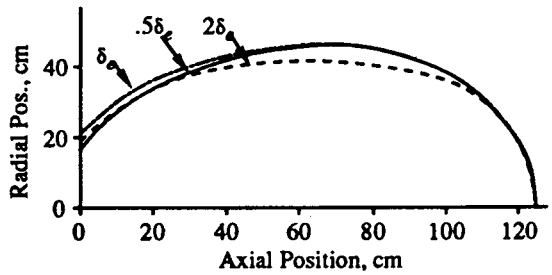

Figure 10(c). - Variation in 1.0×10^{12} mol/cm^3 number density contour with the boundary layer thickness, δ_e

Similarly, the variations in density contours with the selection of α are shown in Fig. 10(b). Varying α affects the solution only in that portion of the plume resulting from the expansion of the boundary layer (angles greater than 31 degrees) since α affects the rate of exponential decay of the plume flow originating from the boundary layer through the parameter β (Eq. *(7)*). The calculations displayed in Fig. 10(b) are for a limiting turning angle of 105 degrees. The model predicts that more flow will go into the backflow region with increasing α.

The effect of boundary layer thickness was also investigated. This parameter determines the location of the

transition from core to boundary layer flow (Eq. *(6)*). It also controls the rate of exponential decay in the plume flow originating in the boundary layer through the parameter β. In this analysis, the boundary layer thickness was determined using a flat plate analysis and was calculated to be on the order of 25% of the exit area. Number density contours were calculated for boundary layer thicknesses twice the calculated value and one half the calculated value. The variation in the calculated contours is shown in Fig. 10(c) for $\alpha = 1.0$ and $\theta_\infty = 105$ degrees. These calculations show that the model is not sensitive to the value of δ_e for the given flow conditions.

The above discussion implies that the selection of α and θ_∞ is critical in comparing theory and experimental values. These functional dependencies also indicate that measured values in the plume can provide insight into conditions at the nozzle exit plane.

Comparison of Model with Experiment

A comparison of the experimental values of mass flux and those from the analyses is made in Fig. 11. The dashed lines in the figure were generated from a linear interpolation scheme of the measured mass flux. The solid lines in the figure were determined based on number densities calculated using the modified Simons' method and values of the critical plume parameters which gave the best agreement with the experimental values. Conversion of the calculated number density values to mass flux requires the particle velocity. The calculated limiting velocity was chosen. This velocity was calculated assuming the nozzle flow expanded to zero static pressure. The limiting velocity used to convert the calculated density to mass flux was 1660 m/s. The difference between the gas velocity based on measured specific impulse and the calculated limiting velocity was less than one percent. The values of all variables used in the analysis are listed in Table III. The agreement between the measured and calculated values is excellent.

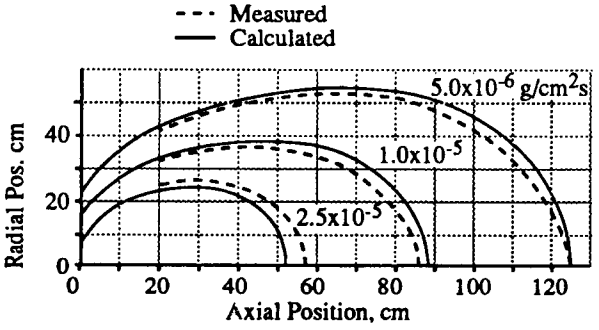

Figure 11. - Measured and Calculated Mass Flux Contours

Table III - Input Parameters

Plume normalization constant, A	9.76×10^{-1}
Nozzle throat radius, R^*	3.8×10^{-2} cm
Nozzle exit radius, r_e	3.8×10^{-1} cm
Limiting velocity, U_{lim}	1660 m/s
Limiting velocity in the boundary layer, $\bar{U}_{lim}$	1660 m/s
Ratio between U_{lim} and $\bar{U}_{lim}$, α	1.0
Plume parameter, β	5.69
Specific heat ratio, γ	1.33
Boundary layer thickness, δ_e	9.95×10^{-2} cm
Angle to edge of boundary layer, θ_o	44°
Limiting turning angle, θ_∞	105°
Nozzle throat density, ρ^*	3.85×10^{-4} g/cm^3

The excellent agreement between the calculated values and the measured values indicate that the Simons' source flow approximation is a viable tool for predicting the exhaust from a liquid-fed water resistojet. The 105 degree limiting turning angle indicated that the plume expanded more than anticipated. This was the result of either backscatter from the forward portion of the plume, or a significant subsonic boundary layer that was neglected in the analysis, or a much lower exit plane Mach number than calculated. It must be stressed that experimental data are required to define nozzle conditions before accurate plume calculations can be made. In particular, the value of the exit Mach number is critical as it defines the limiting turning angle.

CONCLUDING REMARKS

This paper has presented an experimental and analytical investigation of the exhaust from a liquid-fed water resistojet. The resistojet was operated at a mass flow rate of 0.1 g/s with a heater input of 330 W. Mass flux measurements were taken throughout the forward flow field using a cryogenically-cooled quartz crystal microbalance (QCM). In consideration of the potential impact to sensitive spacecraft surfaces, the surface temperature at which water began to condense was determined as a function of the incident mass flux. Condensation temperatures between 168 and 186 K were measured at various locations in the plume.

Complete rotary surveys were also obtained with the QCM. As has been demonstrated with pure gas expansions into vacuum, a cosine variation was exhibited about the flow streamline. The relationship between mass flux and flow angle was employed to obtain data at higher density regions of the plume where the dynamic range of the QCM was exceeded. Data were taken at a known angle to an assumed streamline and corrected to obtain the appropriate value of mass flux. In total, QCM measurements were taken at over sixty locations in the plume on both sides of the thrust centerline. The resistojet plume was axi-symmetric; however, the rotary surveys with the QCM indicated differences in the background levels of mass flux on either side of the plume centerline due to non-uniform pumping in the vacuum tank. Evidence of pressure gradients in the tank were documented with the QCM measurements and also with pressure gauges.

Finally, the mass flux data were compared to theoretical predictions based on a modified version of Simons' method. Excellent agreement between theory and experiment was attained; however, a careful selection of several critical plume parameters was required. The sensitivity of the calculated density contours on three plume parameters was discussed.

REFERENCES

1. Jones, R.E., Morren, W.E., Sovey, J.S. and Tacina, R.R., "Space Station Propulsion," NASA TM-100216, Dec. 1987.

2. Louviere, A.J., Jones, R.E. Morren, W.E., and Sovey, J.S., "Water-Propellant Resistojets for Man-Tended Platforms," IAF 87-259, Oct. 1987, (NASA TM-100110).

3. Stone, J.R., "NASA Electrothermal Auxiliary Propulsion Technology," NASA TM-87271, June 1986.

4. Greco, R.V. and Bliss, J.R., "Resistojet Systems Studies Directed to the Space Station/Space Base, Vol. I - Station/Base Resistojet System Design," (MDC-

G2125, McDonnell Douglas Astronautics Co.; NASA Contract NAS1-10127) NASA CR-111879, April 1971.

5. Suebold, J.G., "Use of Viscous Nozzle Flow Program and the Method of Characteristics Plume Program to Predict Plume Expansion in the Back Flow Region for Small Thrusters," JANNAF 9th Plume Technology Meeting, Chemical Propulsion Information Agency, Laurel, MD, CPIA-PUBL-277, 1976, pp.1-14.

6. Cooper, B.P., "A Computational Scheme Usable for Calculating the Plume Backflow Region," 10th Space Simulation Conference, New York, AIAA, 1978, pp. 150-152.

7. Bird, G.A., "Breakdown of Continuum Flow in Resistojets and Rocket Plumes," 12th International Symposium on Rarefied Gas Dynamics, S.S. Fisher, ed., AIAA, New York, 1980, pp. 681-694.

8. Boyd, I.D. and Stark, J.P.W., "Modelling of Small Hydrazine Thruster Plumes Using Discrete Particle and Continuum Methods," AIAA-88-2631, June 1988.

9. Riley, B.R. and Scheller, K.W.,"Kinetic Theory Model for the Flow of a Simple Gas from a Two-Dimensional Nozzle," 16th International Symposium on Rarefied Gas Dynamics Proceedings, December, 1988.

10. Chung, C. and De Witt, K.J., "Rarefied Gas Flow Through Two-Dimensional Nozzles," AIAA-89-2893, July 1989.

11. Simons, G.A., "Effect of Nozzle Boundary Layers on Rocket Exhaust Plumes," *AIAA Journal*, Vol. 10. No. 11, Sept. 1972, pp. 1534-1535.

12. Genovese, J.E., "Rapid Estimation of Hydrazine Exhaust Plume Interaction," AIAA-78-1091, July 1978.

13. Calia, V.S. and Brook, J.W., "Measurements of a Simulated Rocket Exhaust Plume Near the Prandtl-Meyer Limiting Angle," *J Spacecraft and Rockets*, Vol.12, No.4, April 1975, pp.205-208.

14. Bailey, A.B., Price, L.L., McGregor, W.K. and Matz, R.J., "Flow Field Mapping of Gas/Particle Nozzle Expansion Into Vacuum," AEDC-TR-84-38, July 1985.

15. Bailey, A.B.and Price, L.L. "Flow Field Mapping of Carbon Dioxide Nozzle Expansion Into Vacuum," AEDC-TR-85-26, July 1985.

16. Zana, L.M., Hoffman, D.J., Breyley, L.R., and Serafini J.S., "An Analytical and Experimental Investigation of Resistojet Plumes," NASA TM-88852, Jan. 1987.

17. Hoffman, D.J., "Resistojet Plume and Induced Environment Analysis," NASA TM-88957, May 1987.

18. Breyley, L.R., Hoffman, D.J., Zana, L.M., and Serafini, J.S., "Effect of Nozzle Geometry on the Resistojet Exhaust Plume," AIAA-87-2121, June 1987.

19. Schlichting, H., Boundary Layer Theory, McGraw Hill, New York, 1979, p. 140.

20. Morren, W.E. and Stone J.R., "Development of a Liquid-Fed Water Resistojet," AIAA-88-3288, July 1988, (NASA TM-100927).

21. Chirevella, J.E.,"Hydrazine Engine Plume Contamination Mapping," AFRPL-TR-75-16, Oct. 1975.

22. Brown, R.F. and Wang, E.S., "Capture Coefficients of Gases at 77° K," Advances in Cryogenic Engineering, Vol. 10, K.D. Timmerhaus, Plenum, New York, 1964, pp.283-291.

NASA
National Aeronautics and Space Administration

Report Documentation Page

1. Report No.	2. Government Accession No.	3. Recipient's Catalog No.
NASA TM-102310 AIAA-89-2840		

4. Title and Subtitle	5. Report Date
Investigation of a Liquid-Fed Water Resistojet Plume	
	6. Performing Organization Code

7. Author(s)	8. Performing Organization Report No.
D.H. Manzella and L.M. Carney	E-5005
	10. Work Unit No.
	506-42-31

9. Performing Organization Name and Address	11. Contract or Grant No.
National Aeronautics and Space Administration Lewis Research Center Cleveland, Ohio 44135-3191	
	13. Type of Report and Period Covered
	Technical Memorandum

12. Sponsoring Agency Name and Address	14. Sponsoring Agency Code
National Aeronautics and Space Administration Washington, D.C. 20546-0001	

15. Supplementary Notes

Prepared for the 25th Joint Propulsion Conference cosponsored by the AIAA, ASME, SAE, and ASEE, Monterey, California, July 10-12, 1989. D.H. Manzella, Sverdrup Technology, Inc., NASA Lewis Research Center Group, Cleveland, Ohio 44135; L.M. Carney, NASA Lewis Research Center.

16. Abstract

Measurements of mass flux and flow angle were taken throughout the forward flow region of the exhaust of a liquid-fed water resistojet using a quartz crystal microbalance (QCM). The resistojet operated at a mass flow rate of 0.1 g/s with a power input of 330 Watts. Measured values were compared to theoretical predictions obtained by employing a source flow approximation. Excellent agreement between predicted and measured mass flux values was attained; however, this agreement was highly dependent on knowledge of nozzle flow conditions. Measurements of the temperature at which the exhaust condensed on the QCM were obtained as a function of incident mass flux.

17. Key Words (Suggested by Author(s))	18. Distribution Statement
Resistojets Electrothermal thruster Plumes Contamination steam	Unclassified – Unlimited Subject Category 20

19. Security Classif. (of this report)	20. Security Classif. (of this page)	21. No of pages	22. Price*
Unclassified	Unclassified	10	A03

NASA FORM 1626 OCT 86

*For sale by the National Technical Information Service, Springfield, Virginia 22161